Electronic Structures and Adsorption Properties of Bimetallic Sub-Nanoclusters Pd_xAl_y

การศึกษาโครงสร้างทางอิเล็กตรอนและสมบัติการดูดซับของ Pd_xAl_y

*Sarayute Chansai (สรายุทธ์ จันทร์ช้าย)**

*Dr. Sunantha Hengrasmee (ดร. สุนันทา เฮงรัศมี)***

*Wirach Wongphathanakul (วิรัช ว่องพัฒนากุล)****

*Dr. Konstantin M. Neyman *****

*Dr. Notker Rösch ******

ABSTRACT

The electronic structures and adsorption properties of Pd-Al bimetallic clusters have been theoretically investigated by using an all-electron scalar relativistic density functional method. The nanoscale Pd_{55}, Pd_{79}, and Pd_{116} clusters with O_h symmetry point group were selected to model Pd-Al bimetallic clusters. The presence of Al atoms introduced stabilization of bimetallic clusters, the average cohesive energy per atom increased when Pd atoms were replaced by Al atoms. Al atoms preferentially occupied surface layer and second sublayer of the clusters to produce well distributed alloy. Stabilization led to downwards movement of total d-band center. The adsorption properties of Pd-Al bimetallic clusters relative to the pure Pd clusters have been studied using carbon monoxide as a probe molecule adsorbed on three-fold hollow sites of the (111) facets. The calculated CO adsorption energies and vibrational CO frequencies demonstrated the weakening of the adsorbate-substrate interactions in the presence of Al atoms in the clusters.

บทคัดย่อ

ได้ศึกษาโครงสร้างทางทฤษฎีของการกระจายอิเล็กตรอนและสมบัติการดูดซับของกลุ่มอะตอมโลหะผสมพัลลาเดียม-อลูมิเนียม ด้วยการคำนวณฟังก์ชันความหนาแน่นนโดยใช้อิเล็กตรอนทั้งหมด กล่มอะตอมพัลลาเดียมที่ใช้ประกอบด้วยอะตอมพัลลาเดียม 55 79 และ 116 อะตอม ที่มีโครงสร้างแบบทรงแปดหน้า และได้ศึกษาอะตอมของโลหะผสมที่ถูกสร้างขึ้นโดยการแทรกอะตอมอลูมิเนียมเข้าแทนที่อะตอมพัลลาเดียมในบาตำแหน่ง ผลการคำนวณพบว่าอลูมิเนียมเหนี่ยวนำให้ผลึกมีความเสถียรมากขึ้น โดยมี

Key Words : density functinal calculation, Pd/Al alloy

คำสำคัญ : การคำนวณฟังก์ชันความหนาแน่น โลหะผสมพัลลาเดียม-อลูมิเนียม

---

* *Master student,Master of Science in Chemistry, Department of Chemistry, Faculty of Science, Khon Kaen University*

** *Associate Professor, Department of Chemistry, Faculty of Science, Khon Kaen University*

*** *Assistant Professor, Department of Chemistry, Faculty of Science, Khon Kaen University*

**** *Department de Química Física, Universitat de Barcelona, C/Marti i Franques 1, 08028 Barcelona, Spain.*

***** *Institut für Physikalische und Theoretische Chemie, Technische Universtät München, 85747 Garching, Germany.*

พลังงานยึดเหนี่ยวเฉลี่ยต่ออะตอมเพิ่มขึ้น นอกจากนี้ยังพบว่าอะตอมอลูมิเนียมจะกระจายตัวอยู่ในชั้นของพัลลาเดียมทั้งบนผิวหน้าและชั้นใต้ผิวหน้า เพื่อสร้างโลหะผสมที่มีการกระจายอย่างสม่ำเสมอ ความเสถียรดังกล่าวนี้ทำให้กึ่งกลางของระดับพลังงานออร์บิทัล d ลดระดับลง เมื่อศึกษาสมบัติการดูดซับของกลุ่มอะตอมโลหะผสมพัลลาเดียม-อลูมิเนียมเปรียบเทียบกับกลุ่มอะตอมพัลลาเดียมบริสุทธิ์ โดยให้คาร์บอนไดออกไซด์เป็นโมเลกุลที่ดูดซับลงบนพัลลาเดียม 3 อะตอมที่อยู่กึ่งกลางผิวหน้า พบว่าพลังงานดูดซับลงลดและความถี่ของการสั่นแบบฮาร์โมนิกของคาร์บอนมอนอกไซด์เพิ่มขึ้นซึ่งแสดงถึงอันตรกิริยาที่อ่อนลงระหว่างคาร์บอนมอนอกไซด์กับพื้นผิว เมื่อมีอะตอมอลูมิเนียมแทรกอยู่ในกลุ่มอะตอมพัลลาเดียม-อลูมิเนียม

Introduction

Nanostructures and nanomaterials attract more and more attention as an active field of research because of their outstanding physical and chemical properties. Heterogeneous catalysis, for instance, is an area where nanoparticles have technically been utilized for a long time. This is very important in the chemical industry and in other technologically relavant applications such as oil refinery, organic synthesis, depollution, and so on.

Nowadays, bimetallic or alloy surfaces have become an active field in surface science because they also play a central role in nanotechnology and catalysis. It is well known that the bimetallic catalysts often show enhanced chemical reactivity and selectivity that are different from the corresponding to monometallic ones (single-crystal surfaces). Research on bimetallic catalysts started in the late 1940s with the purpose of investigating the changes that occur in the electronic and adsorption properties.

Previously, the several researches have been focused on the electronic properties of the palladium nanoparticles supported on thin alumina (Pd/Al_2O_3) (Firck et al 1988; *Jiang et al* 1889). Likewise, Carbon monoxide (CO) is the main poisoning intermediate in car-exhaust converter. Therefore, the properties of CO adsorption based on the oxidation of CO have also been investigated. However, the supported catalysts are somewhat difficult to study because of its complexity. To best understand the catalytic behavior of them, we need to use well-defined and simple models, so-called model catalysts (Yudanov et al, 2002).

As mentioned above, we are interested in the cuboctahedral Pd-Al bimetallic clusters representing the Pd supported on thin alumina. Likewise, no previous theoretical study at high level calculation has been reported on the electronic and adsorption properties of Pd-Al bimetallic cluster. Therefore, we will investigate not only the effects of substitution of Pd by Al atoms at various positions and for different the cluster sizes, we will also study their adsorption complexes with CO molecules.

In the current work, we have selected the cuboctahedral Pd_{55}, Pd_{79}, and Pd_{116} clusters to model Pd-Al bimetallic clusters with aluminium substituted at various positions and concentrations by means of all-electron relativistic density functional (DF) calculation. It is well known that CO is widely used as a specific probe molecule for the surfaces of both metal and alloy catalysts. Therefore, the adsorption property is also observed by allowing eight CO molecules to adsorb at three

fold hollow Pd_3 central site of each of the (111) facets. This paper extends the application of novel computational strategy to investigate surface properties of metals and alloys by employing three-dimensional cluster models. A major goal of this work is to study the influence of Al admixtures to Pd clusters on the electronic structure and on their CO adsorption properties.

Computational Details and Method

The calculations reported in this paper were carried out with the all-electron level using the linear combination of Gaussian-type orbital fitting functions density functional (LCGTO-FF-DF) approach as implemented in the parallel code ParaGuass. We also used a scalar relativistic variant of the LCGTO-FF-DF method. This computational strategy is very economic, yet sufficiently accurate for geometric parameters, binding energies, and vibrational frequencies.

The Gaussian type orbital basis set used for Pd and Al atoms was [18*s*, 13*p*, 9*d* / 7*s*, 6*p*, 4*d*] and [12*s*, 9*p*, 2*d* /6*s*, 4*p*, 2*d*], respectively. Whereas [14*s*, 9*p*, 4*d* / 6*s*, 5*p*, 2*d*] was used for both C and O atoms. For every atom, the p and d "polarization exponents" were included as well.

Based on electron configuration of Al atom ([Ne] $3s^2$ $3p^1$), Al atom shows unpaired electron (open-shell configuration). However, the amount of Al atoms containing in the all Pd-Al bimetallic clusters is even number. Therefore, we will discuss only results of spin-restricted calculations. For the investigations of CO adsorption properties, we kept all Pd and Al atoms at positions corresponding to bare cluster. We optimized only the position of adsorbed CO molecules to obtain the approximate equilibrium geometries of adsorption complexes. For that, we consecutively varied Pd-C and C-O distances until deviations were below 0.5 pm by using BP energies. We also corrected the CO adsorption energy for the basis set superposition error via the standard counterpoise technique. To investigate the harmonic CO stretching vibrational frequency, we approximated the C-O internal mode by keeping the CO center of mass fixed. For this purpose, we fitted a polynomial of degree 4 to five total energy values nearby the minimum of the potential curve.

In this paper, the different Pd-Al bimetallic clusters have been employed to carry out a high level study for a wide range of the substitution of Pd by Al atoms. We explored a series of cuboctahedral bimetallic clusters - $Pd_{79-n}Al_n$ (n = 6, 12, 18, 24, 30) as shown in Figure 1. Since all the cluster models revealed a high symmetry belonging to symmetry group O_h, we kept the metal - metal distances in the Pd-Al bimetallic cluster fixed corresponding to Pd-Pd bulk distance of 275 pm (Lide, 1996).

In constructing cluster models, the cuboctahedral clusters M_{79} was obtained by

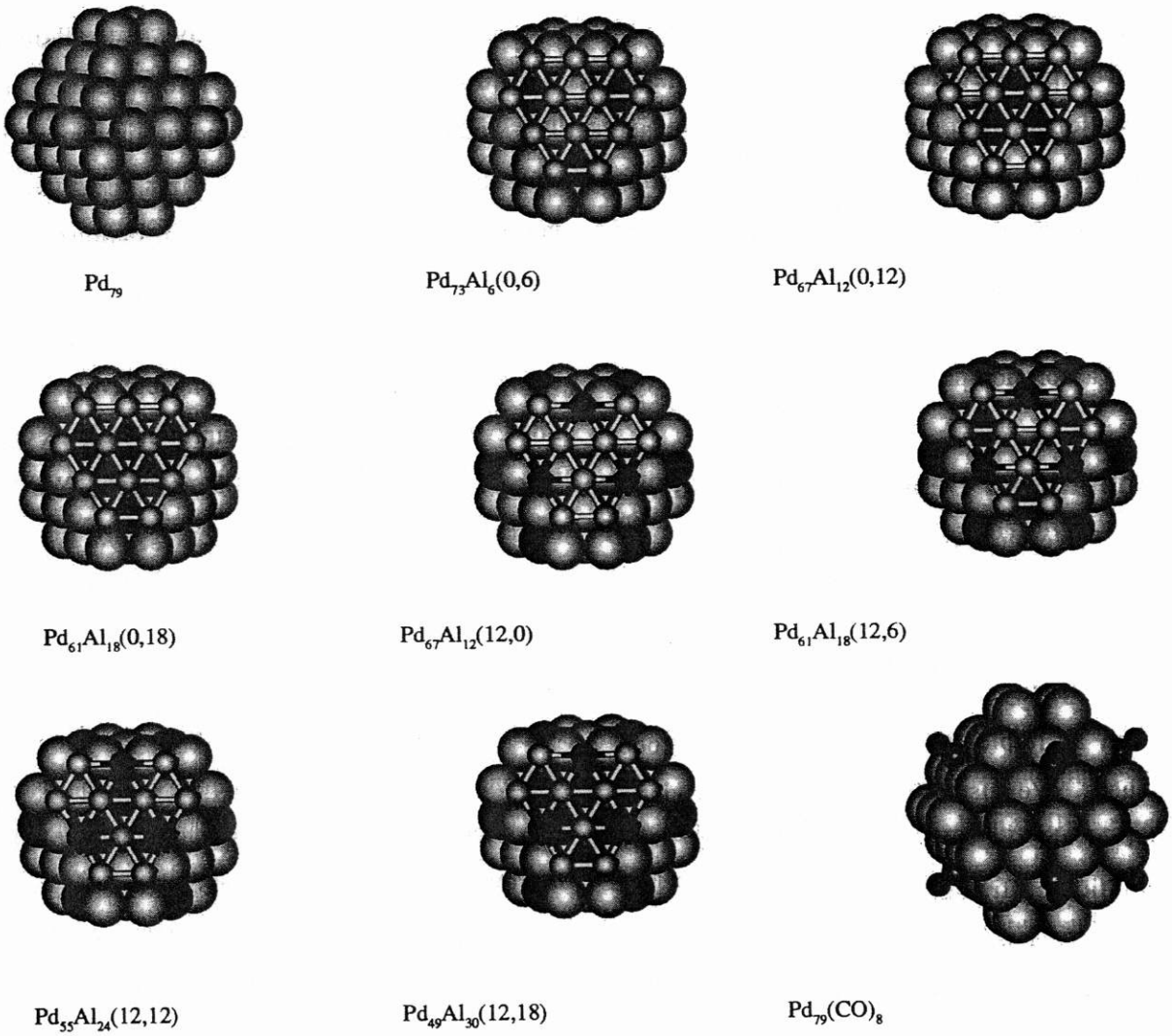

Figure 1 Sketches of the cuboctahedral clusters. The numbers of Al atoms in the surface and sub-surface layer, respectively, are given in parentheses. $Pd_{79}(CO)_8$ model represents the CO adsorption complex.

truncating the corresponding octahedral clusters M_{85} along the planes (100), (010), and (001) to yield eight hexagonal (111) facets. The six corner atoms of M_{85} cluster were removed to provide M_{79} cluster containing also six smallest (001) facets comprised of 4 atoms. This cluster model was designed to represent the (111) surfaces by exhibiting the three fold hollow sites in the center of each (111) facet. This is face centered cubic, fcc, site (with subsurface octahedral hole beneath the site). Adsorption site on these flat facets are rather close to edges. From both experimental and theoretical investigations, it is known that the three-fold hollow site on the Pd (111) surface is favored for CO adsorption at low coverage. Therefore, keeping in mind the low concentration of Al in the bimetallic clusters under investigation, we probed this site by placing CO molecule perpendicular to the (111) surface with the C atom interacting directly with Pd atoms located at the centre of the cluster models.

As described above, we kept intact the central Pd_3 adsorption site on surface layer of each of the eight (111) facets in all Pd-Al bimetallic clusters, but we partially substituted Al atoms for nearby Pd_3 adsorption site. The resulting series of cuboctahedral Pd-Al cluster consist of the following seven bimetallic systems : $Pd_{73}A_{16}(0,6)$, $Pd_{67}Al_{12}(0,12)$, $Pd_{61}Al_{18}(0,18)$, $Pd_{67}Al_{12}(12,0)$, $Pd_{61}Al_{18}(12,6)$, $Pd_{55}Al_{24}(12,12)$, and $Pd_{49}Al_{30}(12,18)$. In designating the cluster models, we used the parenthesis to indicate the number and position of Al atoms. The first number in parenthesis r epresents the number of Al atoms in the top most surface layer and the second one for the inner subsurface layer. In $Pd_{67}Al_{12}(12,0)$ models, each Al atoms are located in the surface layer adjacent to the adsorption site whereas the Al atoms of $Pd_{73}A_{16}(0,6)$, $Pd_{67}Al_{12}(0,12)$, $Pd_{61}Al_{18}(0,18)$ models are in the subsurface layer (inner shell) beneath the central Pd3 adsorption site. For $Pd_{61}Al_{18}(12,6)$, $Pd_{55}Al_{24}(12,12)$, and $Pd_{49}Al_{30}$ (12,18) models, Al atoms are located in both surface layer and subsurface layer.

Results and Discussion

In this section, we will consider the electronic structure of bare $Pd_{79-n}Al_n$ bimetallic clusters relative to pure Pd_{79} cluster used as a reference. Then, we will discuss the CO adsorption properties of these bimetallic ones.

1. Properties of Bare Pd-Al Clusters

Alloying Pd with Al atoms provides the varying numbers of homo- and heteroatomic nearest-neighbor M-M bonds. The interpretation of the heterometallic bonds allows us to better understand the nature of bimetallic bonding in several experimental observations. The calculated characteristics of bare Pd-Al bimetallic clusters are shown in Table 1. Due to various homo- and heterometallic bonds formed in the Pd-Al clusters, the average cohesive energy per atom, E_b / 79, increases when compares with the value obtained for the pure Pd_{79} cluster. Likewise, it seems to increase with the increasing of the number of Pd-Al bonds. This indicates that Al stabilizes the Pd-Al cluster and makes them less reactive to adsorbed species. Those Al atoms tend to distribute themselves among Pd atoms in order to form well distributed alloy. The segregation is not preferred. If one examines the average cohesive energy per bond containing in the clusters, $E_b/336$, one can see that the average cohesive energy per bond of pure Pd_{79} cluster, 0.69 eV, is slightly higher in energy than that of pure Al_{79} one, 0.68 eV. Moreover, the average cohesive energy per bond of all Pd-Al clusters is much higher in energy than those corresponding to both pure Pd_{79} and Al_{79} clusters as can be seen in Table 1. Based on these results, it is indicated that in the Pd-Al

Table 1 Calculated energies a (in eV) for model nanoclusters $Pd_{79-n}Al_n$ (n = 0, 6, 12, 18, 24, 30) along with the number N of the different types of nearest-neighbor contacts (bonds).

	Pd_{79} I	$Pd_{73}Al_{16}$ (0,6)	$Pd_{67}Al_{12}$ (12,0)	$Pd_{67}Al_{12}$ (0,12)	$Pd_{61}Al_{18}$ (12,6)	$Pd_{61}Al_{18}$ (0,18)	$Pd_{55}Al_{24}$ (12,12)	$Pd_{49}Al_{30}$ (12,18)
E_b / 79	2.93	3.15	3.26	3.20	3.45	3.28	3.42	3.47
E_b / 336	0.69	0.74	0.77	0.75	0.81	0.77	0.80	0.82
ΔE_b / n	-	2.91	2.18	1.78	2.30	1.53	1.63	1.42
ΔE_b / N(Pd-Al)	-	0.24	0.31	0.25	0.27	0.23	0.25	0.24
N(Pd-Pd)	336	264	252	240	180	168	144	96
N(Pd-Al)	-	72	84	96	156	120	156	180
N(Al-Al)	-	-	-	24	-	48	36	60
ε_F	-5.10	-5.10	-4.81	-5.06	-4.67	-5.12	-4.81	-4.80
$\Delta\varepsilon_{Pd4d}$	-1.88	-1.82	-1.99	-1.76	-2.07	-1.79	-2.14	-2.22
$\Delta\varepsilon_{Pd4d}(Pd_3)$	-2.03	-1.92	-2.22	-2.27	-2.27	-2.35	-2.50	-2.65

[a] E_b/79 - average cohesive energy of $Pd_{79-n}Al_n$ per atom, E_b/336 (average cohesive energy of $Pd_{79-n}Al_n$ per bond, ΔE_b / n - average contribution of each of the n Al atoms to the change of the overall cohesive energy $E_b(Pd_{79-n}Al_n)$ with respect to $E_b(Pd_{79})$, $\Delta\varepsilon$ Pd_{4d} and $\Delta\varepsilon$ $Pd_{4d}(Pd_3)$ - the centers of the Pd 4*d* density of states with respect to the cluster Fermi energy (F, total and local (for the Pd_3 moiety in the center of (111) facets), respectively.

clusters, the heteroatomic Pd-Al bonding interactions are somewhat stronger than the homoatomic Pd-Pd bonding ones.

Upon investigating the charge distribution at the Pd_3 adsorption site, we find out that the atomic charge at this site varies between positive and negative values. Based on atomic electronegativity values (Pd 1.35, Al 1.47 Allred-Rochow scale), Al atoms could acquire electron density. Nevertheless, the electronegativity of Al atom is somewhat close to that of Pd atom. It, therefore, is expected that electrons may transfer either from Al atom to Pd atom or from Pd atom to Al atom. This transfer depends on the specific structural environment of each atom. Thus, the substitution of Pd by Al

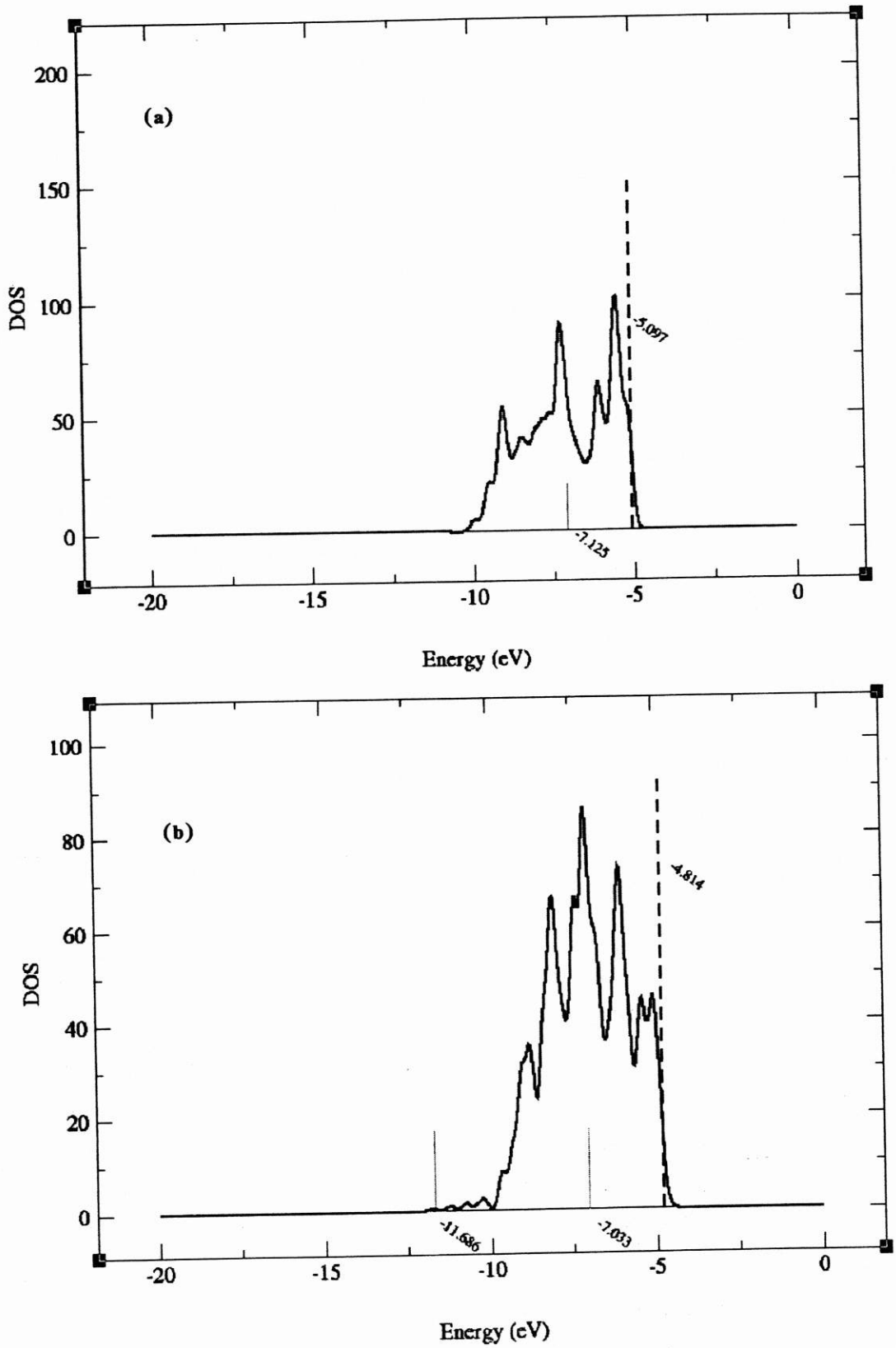

Figure 2 Local (Pd_3 adsorption site) density of states (LDOS) for surface Pd atoms in Pd_{79} cluster **(a)** and in $Pd_{67}Al_{12}$ (0,12) cluster **(b)**. The dashed and dotted vertical lines refer to Fermi level and Pd 4*d*-band center, respectively.

atom at the different positions gives difference effects on the distribution of electrons at Pd_3 adsorption site. However, we need to investigate the density of states (DOS) that provide the distribution of electron in energy. This will be discussed below.

One of the important parameters investigating the electronic structure is the Fermi energy, $\varepsilon_{F.}$ There are three clusters that exhibit Fermi energy closer to the Fermi energy of Pd_{79} clusters. These are $Pd_{73}Al_6$ (0,6), $Pd_{67}Al_{12}$ (0,12), and $Pd_{61}Al_{18}$ (0,18). The mixing of d electrons of Pd with sp electrons of Al underneath shifts (F toward lower energy and electrons are less diffuse, On the other hand, for the others as shown in Table 1, the mixing of d electrons of Pd with sp electrons of Al at surface layer moves (F towards higher energy and electrons are more diffuse relative to those of the reference Pd_{79} clusters.

Additionally, the center of Pd 4*d*-band is widely used to characterize the ability of the adsorbate-surface bonding interaction. Figure 2 shows some of the local (Pd_3 adsorption site) density of states (LDOS) of the surface Pd atoms. For Pd-Al clusters, the Pd 4*d* band of Pd_3 adsorption site is broader than that of pure Pd_{79} clusters. The DOS plot of all Pd-Al clusters demonstrates the major d-band and small peaks around -10.2 eV. These small peaks are the energy level that indicates the mixing of electron between the Pd d band and Al sp band. This slightly destabilizes the center of Pd 4*d*-band. The 4*d*-band centers of total Pd atoms with respect to (F shifts away from those corresponding to pure Pd_{79} clusters. They are separated into two groups. The first group that shifts upwards consists of $Pd_{67}Al_{12}$ (0,12), $Pd_{73}Al_6$(0,6), and $Pd_{61}Al_{18}$(0,18). This group has Al atoms in the second layer only. The second group that shifts downwards has Al atoms at both the surface layer and the second layer. As indicated earlier that having Al in both layers will make the Pd-Al clusters more stabilized and this is consistent with the downward movement of the total Pd 4*d*-band center. Furthermore, the 4*d*-band centers of Pd_3 adsorption site with respect to $\varepsilon_{F,}$ $\Delta\varepsilon_{Pd4d}(Pd_3)$, shift toward higher energy (away from vacuum). Therefore, one of the reasons for weak CO chemisorption on Pd-Al cluster may be that all local 4*d*-band centers are much below $\varepsilon_{F.}$

2. Properties of CO-Adsorbed Pd-Al Clusters

The interaction of CO with bimetallic surfaces has been the subject of many works because CO is an ideal probe molecule to investigate the chemisorption properties of bimetallic surfaces. Likewise, it can provide a simple test of chemical reactivity as well. There is extensive information about the surface chemistry of this molecule in both monometallic and bimetallic substrates. Also, the bonding mechanism is much better known for CO than for any other simple molecules. The BSSE corrected adsorption energies, geometry parameters, and vibrational CO frequencies are shown in Table 2. The optimized C-O distance varies in narrow

Table 2 Calculated characteristics for adsorption complexes of eight CO molecules on the three fold hollow I sites of the (111) facets of the cuboctahedral Pd-Al bimetallic clusters.

	Pd_{79} I	$Pd_{73}Al_{16}$ (0,6)	$Pd_{67}Al_{12}$ (12,0)	$Pd_{67}Al_{12}$ (0,12)	$Pd_{61}Al_{18}$ (12,6)	$Pd_{61}Al_{18}$ (0,18)	$Pd_{55}Al_{24}$ (12,12)	$Pd_{49}Al_{30}$ (12,18)
r (Pd-C) /pm	204.1	202.1	206.4	206.2	209.8	212.9	211.1	212.9
r (C-O) /pm	119.2	119.2	118.9	118.8	118.4	117.7	118.1	117.6
E_{ad} /eV	1.82	1.19	1.56	1.50	0.79	1.02	1.25	0.96
ω(C-O) /cm^{-1}	1739	1740	1750	1754	1765	1791	1786	1816
ε_F /eV	-5.31	-5.28	-5.04	-5.29	-4.91	-5.30	-4.98	-5.00
$\Delta\varepsilon_{Pd4d}$ /eV	-2.01	-1.86	-2.19	-1.88	-2.24	-1.97	-2.34	-2.37
$\Delta\varepsilon_{Pd4d}(Pd_3)$/eV	-2.40	-2.51	-2.77	-2.56	-2.92	-2.76	-3.04	-3.13

r(Pd-C), r(C-O) - interatomic distances,

E_{ad} - BSSE corrected adsorption energy per CO molecule,

ω(C-O) -harmonic frequency of the CO vibration, and the other notations as defined in Table 1.

interval from 117.6 -119.6 pm. It is elongated by 6 and 7 pm for the calculated and experimental values for free CO molecule, respectively. Whereas the Pd-C distance spreads over a rather wide interval from 202 to 215 pm. This is due to σ donation and π^* back donation interactions with the substrate. Those interactions describe the nature of the chemisorption bond formed between CO and transition-metal surface. It is best described by the mixing of the CO molecular orbital with the metal d-state as illustrated in Figure 3.

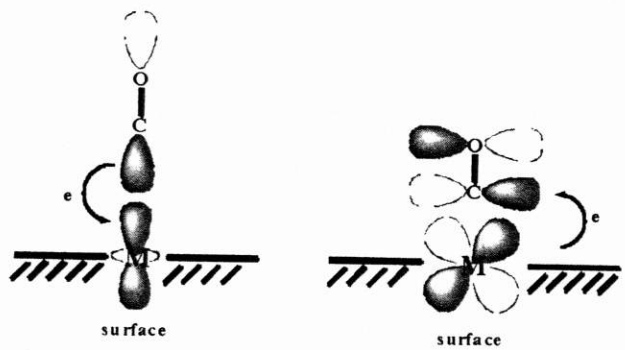

σ donation π back donation

Figure 3 Illustration of orbital interaction between CO and metal surface.

In this model, CO molecule donates electron from its 5σ molecular orbital to vacant metal d-band. This is called σ donation that makes the metal more electron rich. In order to compensate for this extra electron density, a filled metal d-band will interact with $2\pi^*$ antibonding

orbitals of CO. This interaction is called π back donation. Since the CO adsorption on alloy is a complex phenomena, we can simply present the orbital interaction diagram between CO and metal surface as shown in Figure 4.

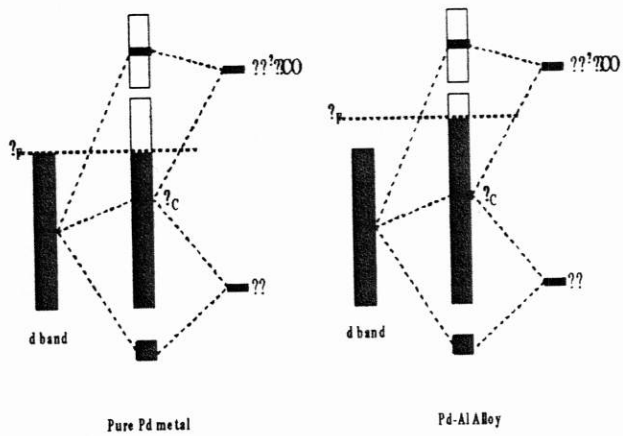

Figure 4 Illustration of orbital interaction between CO and metal surface.

According to Table 2, the Fermi levels of all CO-adsorbed Pd-Al clusters shift toward higher energy. This leads to a broader 4*d*-band of Pd_3 adsorption site. As a consequence, all the 4*d*-band centers of the Pd_3 adsorption site, $\Delta\varepsilon_{Pd4d}(Pd_3)$, shows the downward shift with respect to ε_F. This is illustrated by Figure 4. Due to both σ donation and π back donation, the ε_F is higher in energy. Therefore, the 4*d*-band center of Pd_3 adsorption site, ε_C, is further away from ε_F. This weakens the chemisorption bond between CO and P_3 adsorption site of all Pd-Al bimetallic clusters. Thus, it is shown that the interaction energy is primarily controlled by Pd 4*d*-band energy position. This observation is in agreement with those observed by Hammer et al (1995).

Consequently, if the $2\pi^*$ molecular orbital of CO gains less electrons from Pd 4*d*-band. The π back donation will become weaker. This can lead to a strengthening of C-O bond, which is evidenced by increasing of CO stretching frequency. One can see from Table 2 that the calculated CO vibrational frequencies on various Pd-Al clusters are higher than that on the pure Pd clusters. They spread over a rather wide interval from 1750 to 1816 cm-1. Such a range of CO frequencies, considerably shifted down from the value of gas-phase CO molecule with a calculated harmonic frequency of 2113 cm^{-1}, is typical for CO molecules adsorbed on transition metals.

Interestingly, the substitution of Pd by Al atoms leads to the weakening of CO adsorption energies at Pd_3 adsorption site. The adsorption energy is less than that of CO-adsorbed Pd_{79} cluster with the interval from 1.56 to 0.79 eV. As previously reported, *Johánek et al* (2001) found that the temperature programmed desorption (TPD) spectra of CO adsorption on Pd/Al2O3 exhibit the two desorption peaks located below the desorption temperature of Pd polycrystalline foil. Moreover, the desorption energy compared to that of clean Pd foil is 1.10 eV and 0.98 eV at 405 and 364 K, respectively. As mentioned above, it can be indicated that the adsorption energy of CO adsorption on Pd/Al_2O_3 shows the lower values compared to Pd crystalline foil. Therefore, the calculated results of CO adsorption on Pd-Al clusters are in agreement with the experimental ones.

Conclusion

In the present work, we have presented the theoretical study on the electronic structure of bare Pd-Al bimetallic clusters and on CO adsorption complexes by means of DF calculations. It has

been demonstrated that Pd-Al bimetallic clusters are more stabilized when Al atoms are well distributed among the surface layer and the subsurface of the clusters. Moreover, Pd atoms exhibit the strong interaction with Al atoms by forming a bimetallic alloy with modified electronic structure. For CO adsorption, the calculated CO adsorption energies manifest a weakening of Pd-Al bimetallic surface - CO interactions. Therefore, these Pd-Al bimetallic clusters should be a better catalyst for the reaction involving CO intermediate. The behavior of the bimetallic clusters that is different from the Pd single crystal is due to the changes in the electronic structures. Likewise, more calculations that consider the cluster relaxation and optimization are needed to better understand the Pd-Al interaction and the reactivity of the Pd-Al surface toward CO molecule.

Acknowledgements

We would like to thank Dr. Konstantin M. Neyman and Prof. Notker Rösch for their discussion on this work. Likewise, we gratefully acknowledge the financial support from the Postgraduate Education and Research Program in Chemistry (PERCH).

References

Frick, B., and Jacobi, K. 1988. Growth and Electronic Structure of Ultrathin Palladium Films on Al (111). **Phy. Rev. B** 7: 4408-4414.

Jiang, L.Q., Ruckman, M.W. and Strongin,M. 1989. Experiment Evidence for Room-Temperature Intermetallic Compound Formation at the Pd/Al Interface. **Phys. Rev.** B 39: 1564-1568.

Yudanov., I.V., Sahnoun, R. Neyman, K.M. and R_sch, N. 2002. Metal Nanoparticles as models of Single Crystal Surfaces and Supported Catalysts: Density Functional Study of Size Effects for CO/Pd(111). J. **Chem. Phys.** 117: 9887-9896.

Lide, D.R. 1996. **CRC Handbook of Chemistry and Physics,** 77th edition, CRC Press, Boca Raton.

Hammer, B. and N_rskov, J.K. 1995. Electronic Factors Determining the Reactivity of Metal Surfaces. **Surf. Sci.** 246: 211-220.

Johánek, V., Tsud, N. Matolín, V., and Stará, I. 2001. TPD and XPS Study of the CO Adsoprtion on Transition-SP Metal Systems: Pd and Al. **Vacuum.** 63: 15-22.